Title

The charybdotoxin receptor of a Shaker K+ channel: peptide and channel residues mediating molecular recognition.

Journal

Neuron, 12(6)

ISSN

0896-6273

Authors

Goldstein, SA
Pheasant, DJ
Miller, C

Publication Date

1994-06-01

DOI

10.1016/0896-6273(94)90452-9

The Charybdotoxin Receptor of a *Shaker* K^+ Channel: Peptide and Channel Residues Mediating Molecular Recognition

Steve A. N. Goldstein,* Deborah J. Pheasant, and Christopher Miller
Howard Hughes Medical Institute Graduate Department of Biochemistry Brandeis University
Waltham, Massachusetts 02254

Summary

Charybdotoxin (CTX) is a peptide of known structure that inhibits *Shaker* K^+ channels by a pore-blocking mechanism. Point mutagenesis of all 30 solvent-exposed residues identified the part of the CTX molecular surface making contact with the receptor in the K^+ channel. All close-contact residues are clustered in a well-defined interaction surface; the shape of this surface implies that the outer opening of the *Shaker* channel conduction pore abruptly widens to a 25 x 35 A plateau. A mutagenic scan of the S5-S6 linker sequence of the *Shaker* K^+ channel identified those channel residues influencing CTX binding affinity. The *Shaker* residues making the strongest contribution to toxin binding are located close to the pore-lining sequence, and more distant residues on both sides of this region influence CTX binding weakly, probably by an electrostatic mechanism. Complementary mutagenesis of both CTX and *Shaker* suggests that *Shaker*-F425 contacts a specific area near TB and T9 on the CTX molecular surface. This contact point constrains *Shaker*-F425 to be located at a 20 A radial distance from the pore axis and 10-15 A above the "floor" of the CTX receptor.

Introduction

Charybdotoxin (CTX) belongs to a family of scorpion venom peptides that inhibit voltage-gated and Ca^{2+}. activated K^+ channels (Miller et al., 1985; Gimenez- Gallego et al., 1988; Crest et al., 1992; Possani et al., 1982; Candia et al., 1992; Garcia-Calvo et al., 1993). Acting in the pico-to nanomolar concentration range, these peptides inhibit their molecular targets by a bi- molecular mechanism in which a single toxin molecule binds to a receptor located near the external end of the K^+ conduction pore, thereby blocking K^+ permeation (MacKinnon and Miller, 1988; Giangiacomo et al., 1992; Park and Miller, 1992a; Goldstein and Miller, 1993). The simplicity of the blocking mechanism has allowed these peptides to be used as molecular probes of K^+ channels, pointing to the region of the protein bearing both the CTX receptor and the ion conduction pathway (MacKinnon and Miller,1989; MacKinnon and Yellen, 1990) and demonstrating the tetrameric stoichiometry of the channel complex (MacKinnon, 1991; MacKinnon et al., 1993). In this study, we examine mutants of both CTX and a *Shaker* - type voltage-gated K^+ channel to identify the important points of interaction between toxin and channel.

Detailed NMR studies (Bontems et al., 1991, 1992) have shown that CTX forms a compact globular structure maintained rigid by three disulfide bonds. The peptide's entire internal volume is filled by these 6 cysteine residues, whereas all non-cysteine side chains lie on the surface and project into solvent. These molecular characteristics make CTX particularly well suited for analysis of the roles of individual residues in the toxin-receptor interaction, since they favor the likelihood that point mutants will exert only local effects on toxin binding. This locality of point mutations underlies the utility of CTX as a structural probe of the channel (MacKinnon and Miller, 1989; Park and Miller, 1992a, 1992b; Stampe et al., 1994).

A set of point mutants of CTX was recently used to map the region of the toxin's molecular surface that makes direct contact with the receptor of a high conductance Ca^{2+}-activated K^+ (BK) channel from rat muscle (Stampe et al., 1994). A cluster of 8 residues, forming about 25% of the toxin surface, was identified as the area of intimate contact with the BK channel. We now extend this analysis to a *Shaker* channel, which provides ready genetic manipulability and offers the advantage of a well-

*Present address: Boyer Center for Molecular Medicine, Yale University School of Medicine 295 Congress Avenue, New Haven, Connecticut 06511.

understood molecular architecture (Miller, 1991). The results demonstrate that CTX presents to the *Shaker* K^+ channel an interaction surface similar to that deduced for the BK channel. In addition, by identifying residues on the channel that specifically influence CTX binding, we engineer a CTX receptor site that displays 10^5-fold higher affinity for the peptide than does wild-type *Shaker*. Finally, complementary mutagenesis between the channel and the toxin suggests a specific pair of interaction partners involved in CTX binding to *Shaker* and produces an initial view of the receptor's three-dimensional topography.

Results

Kinetics of CTX Blockade

We examined the effects of CTX point mutations by measuring the association and dissociation rates of toxin with a *Shaker* K^+ channel expressed in Xenopus oocytes, using outside-out macropatches or whole-oocyte, two-electrode voltage clamp. For most measurements, we used an inactivation-removed *Shaker* B channel (6.6-46) with an additional point mutation, F425G, which increases its CTX affinity over 3 orders of magnitude (Goldstein and Miller, 1992, 1993). Figure 1 illustrates the time course of block by a slightly weakened CTX mutant, R34K, using 50 ms observation pulses applied at 15 s intervals. After 4 control pulses, the oocyte was abruptly exposed to toxin (Figure 1A), and progressive block of K^+ current to a new steady- state level ensued. Removal of toxin (Figure 1B) resulted in return of the current to the unblocked level. As described previously (MacKinnon and Miller,1989; Goldstein and Miller, 1993), toxin block proceeded without altering channel activation kinetics; currents simply scale down, since CTX kinetics were much slower than voltage-dependent gating. Both wash-in and wash-out relaxations were well fitted by single exponentials, as previously documented in detail (Escobar et al., 1993; Goldstein and Miller, 1993). For all toxins studied, currents recovered to within 5% of unblocked levels upon wash-out of toxin.

Functional Consequences of CTX Point Mutations

Table 1 summarizes the kinetic behavior of 67 point mutants of CTX made at all 30 solvent-exposed positions. In all cases, kinetics were well behaved as in Figure 1, and the toxin variants satisfied previously established criteria for correctness of folding and of blocking mechanism (Park and Miller, 1992b; Gold- stein and Miller, 1993; Stampe et al., 1994). In nearly all cases, toxin association rates were close to the wild-type value; those mutants showing greatly diminished blocking activity manifested this altered interaction mainly in increased dissociation rates.

Charge Neutralization Mutations

CTX is a basic protein with 8 positively charged and 2 negatively charged groups (including the C-terminus), and a net charge of about +5 at neutral pH (Gimenez- Gallego et al., 1988). The ionic strength dependence of CTX block argues that electrostatic interactions contribute to CTX binding (MacKinnon et al., 1989). Accordingly, in an initial set of experiments, we tested the effects of neutralizing each charged residue to glutamine. Of the 9 mutants made, 7 (K11Q, E12Q, R19Q, H21Q, R25Q, K31Q, and K32Q) produced a small (2- to 13-fold) reduction of binding affinity. Individual mutation of the remaining 2 residues led to large losses in affinity: K27Q (15,000-fold) and R34Q (300-fold). In all cases, these mutations had only mini- mal effects on association rates; even the highly destabilized mutants, K27Q and R34Q, showed association rates within 3-fold of the wild-type value. This pattern of charge neutralization is identical to that seen with the BK channel (Stampe et al., 1994), although the affinity losses for the 2 sensitive residues, K27 and R34, are larger with *Shaker* than with the BK channel.

Classification of Residues

In surveying the mutants in Table 1, we classified resi- dues into three groups according to off-rate effects, which reflect primarily intimate interaction with the channel (Stampe et al., 1994). We

Table 1. Blocking Parameters for Wild-Type and Mutant CTX Isoforms

Position	Mutation	K_D (nM)	k_{on} $\mu M^{-1}s^{-1}$	k_{off} s^{-1}	K_D Ratio (mut/wt)	On-Rate Ratio (mut/wt)	Off-Rate Ratio (mut/wt)
Wild-type	None	0.074 ± 0.004	61 ± 4	0.0046 ± 0.0003	=1	=1	=1
1-PyroGlu	Z1P	42 ± 2	0.86 ± 0.05	0.036 ± 0.003	570	0.01	7.8
2-Phe	F2A	0.19 ± 0.02	38 ± 5	0.007 ± 0.002	2.6	0.6	1.5
	F2W	0.452 ± 0.009	10 ± 1	0.0045 ± 0.0004	6.1	0.2	1.0
	F2E	0.51 ± 0.02	32 ± 2	0.016 ± 0.001	6.9	0.5	3.5
3-Thr	T3L	0.43 ± 0.03	22 ± 2	0.0088 ± 0.0002	5.8	0.4	1.9
4-Asn	N4D	0.23 ± 0.05	16 ± 3	0.0032 ± 0.0004	3.1	0.3	0.7
5-Val	V5E	0.054 ± 0.002	59 ± 2	0.0036 ± 0.0004	0.73	1.0	0.8
6-Ser	S6D	0.27 ± 0.03	23 ± 5	0.0049 ± 0.0003	3.6	0.4	1.1
8-Thr	T8S	0.077 ± 0.007	31 ± 5	0.0022 ± 0.0001	1.0	0.5	0.5
	T8K	0.092 ± 0.01	48 ± 3	0.0044 ± 0.002	1.2	0.8	1.0
9-Thr	T9V	0.13 ± 0.02	37 ± 10	0.0044 ± 0.0005	1.8	0.6	1.0
	T9K	0.078 ± 0.007	48 ± 4	0.0037 ± 0.0003	1.1	0.8	0.8
	T9G,T8S	0.073 ± 0.004	98 ± 6	0.0073 ± 0.0004	1.0	1.6	1.6
10-Ser	S10A	0.267 ± 0.008	46 ± 3	0.012 ± 0.001	3.6	0.8	2.6
	S10T	0.21 ± 0.01	34 ± 4	0.0065 ± 0.0007	2.8	0.6	1.4
	S10Q	0.69 ± 0.05	149 ± 18	0.085 ± 0.006	9.3	2.4	18
	S10D	114 ± 35	ND	ND	1,500	ND	ND
11-Lys	K11Q	0.123 ± 0.007	61 ± 4	0.0072 ± 0.0007	1.7	1.0	1.6
	K11E	0.36 ± 0.004	20 ± 3	0.007 ± 0.001	4.9	0.3	1.5
12-Glu	E12Q,K11Q	0.051 ± 0.002	63 ± 3	0.0032 ± 0.0001	0.7	1.0	0.7
14-Trp	W14A	0.198 ± 0.004	49 ± 6	0.0100 ± 0.0009	2.7	0.8	2.2
	W14M	0.23 ± 0.02	18 ± 3	0.0039 ± 0.0002	3.1	0.3	0.9
15-Ser	S15Y	0.180 ± 0.004	33 ± 5	0.0059 ± 0.0007	2.4	0.6	1.3
16-Val	V16E	0.20 ± 0.03	24 ± 6	0.0039 ± 0.0009	2.7	0.4	0.9
18-Gln	Q18K	0.088 ± 0.007	28 ± 4	0.0023 ± 0.0002	1.2	0.5	0.5
19-Arg	R19Q	0.17 ± 0.01	34 ± 4	0.0058 ± 0.0006	2.3	0.6	1.3
20-Leu	L20N	0.198 ± 0.006	31 ± 4	0.0060 ± 0.0007	2.7	0.5	1.3
21-His	H21Q	0.15 ± 0.02	68 ± 8	0.0099 ± 0.0006	2.0	1.1	2.2
22-Asn	N22K	0.092 ± 0.027	28 ± 3	0.0027 ± 0.0007	1.2	0.5	0.6
23-Thr	T23D	3.6 ± 0.3	15 ± 1	0.052 ± 0.003	49	0.2	11
24-Ser	S24D	0.62 ± 0.05	88 ± 6	0.052 ± 0.002	8.4	1.4	11
	S24K	0.18 ± 0.02	25 ± 1	0.0045 ± 0.0006	2.4	0.4	1.0
25-Arg	R25Q	0.95 ± 0.05	23 ± 2	0.021 ± 0.007	13	0.4	4.6
	R25D	104 ± 3	4.1 ± 0.2	0.401 ± 0.009	1,400	0.1	87
27-Lys	K27Q(SP)	1,200 ± 50	50 ± 4	70 ± 5	16,200	0.8	15,200
	K27R(SP)	104 ± 4	50 ± 4	5.3 ± 0.6	1,400	0.8	1,100
	K27N(SP)	590 ± 80	90 ± 7	70 ± 3	8,000	1.5	15,200
	K27M(SP)	330 ± 8	126 ± 5	34 ± 1	4,500	2.1	7,400
	K27H(SP)	2,200 ± 100	31 ± 1	68 ± 3	30,000	0.5	15,000
	K27S(SP)	4,500 ± 400	7 ± 1	36 ± 5	61,000	0.1	7,800
	K27E(SP)	5,000 ± 300	ND	ND	68,000	ND	ND
	K27D	600 ± 100	0.025 ± 0.003	0.020 ± 0.003	8,100	0.0004	4.3
29-Met	M29I	0.11 ± 0.02	49 ± 11	0.0041 ± 0.0006	1.5	0.8	0.9
	M29L	0.46 ± 0.01	180 ± 10	0.081 ± 0.005	6.2	2.9	18
	M29K	250 ± 13	79 ± 2	23 ± 1	3,400	1.3	5,000
	M29E	>500	ND	ND	>6,800	ND	ND
	M29G	>1 μM	ND	ND	>13,500	ND	ND
30-Asn	N30Q(SP)	115 ± 8	200 ± 12	22.6 ± 0.9	1,600	3.2	4,900
	N30G(SP)	62 ± 4	115 ± 4	7.3 ± 0.3	840	1.9	1,600
	N30D	>275	ND	ND	>3,700	ND	ND
	N30E	>275	ND	ND	>3,700	ND	ND
31-Lys	K31Q	0.39 ± 0.03	38.8 ± 0.1	0.015 ± 0.001	5.3	0.6	3.3
32-Lys	K32Q	0.37 ± 0.04	26 ± 5	0.0090 ± 0.0006	5.0	0.4	2.0
	K32Q,R19Q	0.48 ± 0.02	30 ± 4	0.014 ± 0.002	6.5	0.5	3.0
34-Arg	R34Q	21 ± 1	23 ± 1	0.473 ± 0.007	290	0.4	103
	R34K	0.22 ± 0.02	29 ± 3	0.0060 ± 0.0001	3.0	0.5	1.3
	R34E	>275	ND	ND	>3,700	ND	ND
	R34D	>275	ND	ND	>3,700	ND	ND
36-Tyr	Y36F	0.53 ± 0.05	38 ± 6	0.020 ± 0.004	7.2	0.6	4.3
	Y36L	48 ± 2	8.5 ± 0.8	0.38 ± 0.02	650	0.1	83
	Y36Q(SP)	226 ± 18	160 ± 5	37 ± 2	3,100	2.5	7,900
	Y36N	14.4 ± 0.5	45 ± 2	0.81 ± 0.06	195	0.7	180
	Y36E	>500	ND	ND	>6,800	ND	ND
	Y36A(SP)	154 ± 2	83 ± 3	13.5 ± 0.6	2,100	1.4	2,900
37-Ser	S37Q	0.08 ± 0.02	26 ± 9	0.0017 ± 0.0002	1.1	0.4	0.4
	S37X	0.42 ± 0.03	110 ± 12	0.044 ± 0.004	5.7	1.8	9.4

The dissociation constant (K_D), second-order association rate constant (k_{on}), and first-order dissociation rate constant (k_{off}) were determined in macropatches by the multi-pulse or single-pulse protocol (marked "SP") except for toxin variants F2W, F2E, T3L, N4D, S6D, T8S, T8K, T9V, T9K, S10A, S10T, S10D, K11E, W14M, S15Y, V16E, Q18K, L20N, N22K, S24K, R34K, and S37Q, which were studied in whole-cell clamp using the multi-pulse protocol as described in Experimental Procedures. The values shown are the mean ± SE for 3–22 independent determinations. ND, not done.

defined critical residues as those that, when replaced in a chemically conservative manner, led to off-rate increases greater than 15-fold. Likewise, influential residues are those in which mutations resulted in 3- to 5-fold off-rate increases. Residues that gave less than 3-fold destabilization when replaced in a chemically radical manner were classified as indifferent.

According to this scheme, 5 residues fall into the critical category; 2 of these (K27 and R34) are positively charged, 2 are strongly hydrophobic (M29 and Y36), and 1 (N30) is small and polar. Each of these positions was studied further. The positive charges of the 2 basic residues appeared to be functionally relevant, since R34K was nearly wild type in behavior, and K27R, though 1000-fold destabilized, was the least altered of all mutations made at this most critical position. The 3 other critical positions showed tight structural requirements for maintenance of blocking activity. For instance, isoleucine was tolerated well as a re- placement for M29, but leucine was not; lysine, which can be grossly envisioned as a pseudo-methionine with a positively charged "head," substituted very poorly. Phenylalanine, but not leucine or alanine, substituted effectively at Y36. We have not found any residue that can replace N30 with retention of high affinity block.

In striking contrast to the critical residues are 17 positions, classified as indifferent, that tolerated large variation in side chain identity without effects on dissociation rates: T3, N4, VS, S6, T8, T9, K11, E12, W14, S15, V16, Q18, R19, L20, H21, N22, and K32. We are particularly impressed that some of these could be replaced by charged residues without off-rate effects (e.g., N4D, VSE, S6D, T8K, T9K, V16E, Q18K, and N22K). The insensitivity of toxin block to the chemical nature of these residues is a strong argument that CTX does not contact the channel at these regions of its molecular surface.

The categorization of the 8 remaining solvent-exposed side chains was less clear; their functional behaviors lay between the critical and the indifferent residues, and we have classified these as merely influential. For instance, mutants creating negative charges at 5 of these positions, F2E, S10D, T23D, S24D, and R25D, increased dissociation rates 10-to 100-fold. These are mild effects when compared with substituting negative residues at critical positions (compare with K27E, M29E, N30D, R34D, and Y36E); but they produced much stronger effects than charge replacements at the indifferent positions cited above. Thus, these 5 residues acted as if they were close to, but not in contact with, the channel when the toxin was bound. Likewise, mutations at 3 other positions were notable for their intermediate effects on off-rates. Replacement of the N-terminal pyroglutamate with a praline, a sterically (but not electrostatically) conservative alteration, yielded 8-fold acceleration of the dissociation rate, and truncation of the C-terminal residue (S37X) or replacement of S10 with a larger polar residue (S10Q) caused similar destabilization. On the basis of these and other mutations (Table 1), we classified 8 residues as influential: Z1, F2, S10, T23, S24, R25, K31, and S37.

The CTX Interaction Surface

Figure 2 displays four views of the non-hydrogen van der Waals surface of CTX, in which residues are colored according to the above classification scheme. The 5 critical residues are colored red, the 8 influential residues yellow, and the 17 indifferent residues green. The 6 cysteine residues and glycine 26, all of which are buried in the protein's small internal core (and for this reason were not mutated) are rendered in white.

The major result of this survey is that residues of like color are segregated on the molecular surface. All of the critical red residues lie together in an area of 530 $Å^2$, 17% of the molecular surface. We propose that this represents the toxin's "interaction surf ace" making close contact with the CTX receptor. Likewise, all of the indifferent green residues form a simply connected surface covering over half the molecule (1730 $Å^2$). We did not expect to be able to make any argument about the weakly influential yellow residues, since the behavior of mutations at these positions was equivocal, neither cleanly critical nor indifferent. However, a frontal view of the interaction surface (Figure 2D) rationalizes the intermediate characteristics of these positions: the yellow residues form a 830 $Å^2$ border around the red interaction surface, clearly separating it from the indifferent residues.

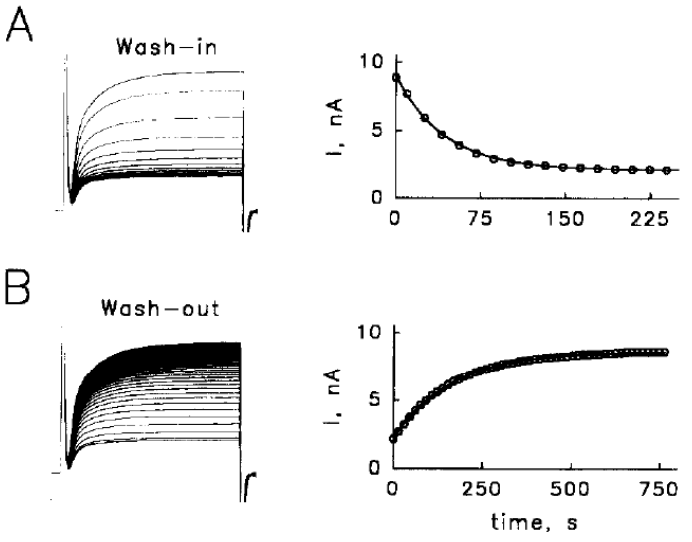

Figure 1. Blockade of K^+ Current by CTX Mutants
Xenopus oocytes expressing *Shaker* channels were studied by two-electrode voltage clamp using a multi -pulse protocol in a perfusion chamber. Oocytes were held at -80 mV and pulsed to0 mV for 50 ms with an interpulse interval of 15 s. (A) Successive pulses after exposure to 0.5 nM R34K. (B) Time course of toxin wash-out. Scale bars represent 1 μA and 7.5 ms. To the right of each experiment is shown a time course of the current measured at 45 ms into each test pulse; single-exponential relaxations are superimposed on the data (smooth curves).

Effects of K^+ Channel Mutations on CTX Affinity

We next examined the CTX receptor in the *Shaker* channel itself. The only part of the sequence of *Shaker* K^+ channels known to contain determinants of the CTX receptor is in the linker between the fifth and sixth transmembrane helices, on the two externally facing ends of the pore-forming P-region. Previous work (MacKinnon and Miller, 1989; MacKinnon et al., 1990; Escobar et al., 1993) identified several residue in this area that, when mutated, destabilize binding of agitoxin, a CTX isoform. We originally confused agitoxin with CTX (MacKinnon and Miller, 1989), but this homolog has now been isolated, sequenced, and shown to differ from CTX in its specificity among K channels (Garcia et al., 1994). We therefore examined all residues in this area for their effects on binding of authentic CTX. We mutated each residue from positions 418-456 (exclusive of the P-region residues 432-447, many of which are unforgiving of mutation) to lysine, or from lysine to aspartate. The rationale for using this series of constructs is that electrostatic forces are known to influence CTX binding at distances on the order of 10 Å (MacKinnon and Miller, 1989). A mutagenic scan employing electrostatically altered channels might therefore be expected to identify not only residues that make close contact with the toxin, but also those that are physically close in space to the CTX receptor.

Of these 24 *Shaker mutants*, 8 failed to express K^+ current. Only 1 of the 16 remaining mutants, M448K, showed significantly altered gating kinetics (rapid C-type inactivation; data not shown), and only 1 (A419K) had no discernable effect on CTX block. Electrostatic mutations at 6 positions (G425, K427, D431, M448, T449, and V451) altered CTX affinity dramatically, 50-fold or greater (Figure 3). Large changes in toxin dissociation rates were observed with all of these strong mutations. Eight mutations weakened CTX block only slightly (2- to 25-fold); 5 of these are located on the N-terminal side of the P-region (G420, 5421, E422, N423, and 5424), and 3 are on the C-terminal side (G452, V453, and W454). CTX block of several of these milder mutations (G420K, E422K, 5424K, G452K, and V453K) was weakened mainly via decreased association rates, with only small effects on dissociation rates. For all mutations, we also assayed affinity of block by externally applied tetraethylammonium (TEA) and found roughly parallel, though much smaller, mutagenic effects on this small, low affinity blocker (Table 2).

Several positions are especially noteworthy for their effects on CTX block. The 15-fold

destabilization resul ting from the mutation E422K was quantitatively identical to the same mutation analyzed for agitoxin binding to wild-type *Shaker* (MacKinnon and Miller, 1989; MacKinnon et al., 1990; Escobar et al., 1993). This channel position influenced CTX binding via a distant electrostatic interaction with the positively charged toxin. The mutation K427D strengthened CTX binding about 50-fold, analogous to its electrostatic strengthening of agitoxin block (MacKinnon et al., 1990). Substitution of lysine at residue 449, a position known as a strong determinant of external TEA binding (MacKinnon and Yellen, 1990), eliminated block by both CTX and TEA. These two blockers bind in a mutually exclusive fashion to CTX receptors (Miller, 1988; Giangiacomo et al., 1992; Goldstein and Miller, 1993), and so it is easy to picture their binding sites as sharing common residues.

The overall picture emerging from this survey agrees with earlier studies using agitoxin (MacKinnon et al., 1990): that numerous residues on both sides of the P-region sequence affect CTX binding and that these effects grow stronger as the deep-pore sequence is approached from either side. This conclusion further corroborates the postulated mechanism of CTX block of K^+ channels: that CTX physically covers the K^+ conduction pathway by binding to a receptor located near its opening to the external solution.

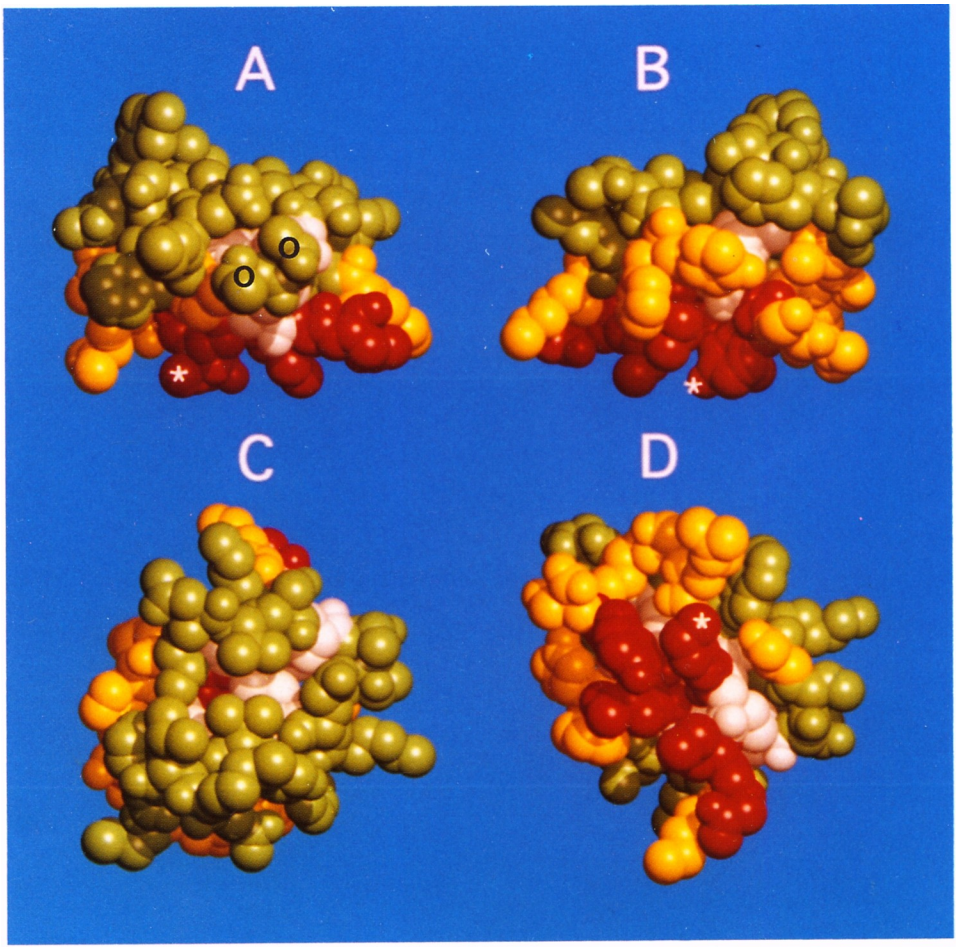

Figure 2. Van der Waals Surface Model of CTX
Four views of the non-hydrogen van der Waals surface is represented from NMR-determined coordinates (Bontems et al., 1992). Coloring is based on the effect of point mutation on toxin off-rate. As defined in the text, critical residues are red, influential residues are yellow, and indifferent residues are green. The white asterisk in each panel indicates the ε-amino group of K27. (A and B) "Front" and "rear" views, respectively. (C) "Top" view. (D) "Bottom" view of interaction surface. The black circles in view (A) represent the residues T8 and T9.

Steric Interactions Studied by Complementary Mutagenesis

The residue at *Shaker*-425 was studied in additional detail because of its special influence on the affinity and selectivity of the CTX receptor of voltage-gated K^+ channels. Phenylalanine resides at this position

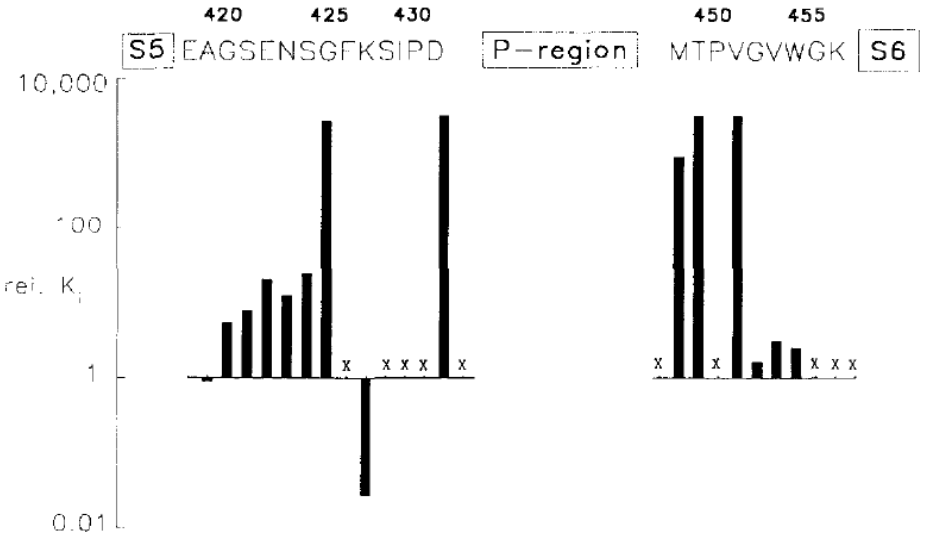

Figure 3. A Mutagenic Scan of the CTX Receptor Sequence

Point mutants were constructed in which each residue of the S5- S6 linker sequence (above) was replaced by lysine, except for the natural lysine (position 427), which was replaced by aspartate, and excluding the P-region position s 432-446. Closed bars show the dissociation constant of CTX tested on each mutant, relative to its value (74 pM) measured on the *Shaker* channel used here. Mutants that failed to express K^+ current are marked with X. Relative values of association and dissociation rates, respectively, for mutants at selected positions are as follows. E422K: 0.07, 0.9; 5424K: 0.07, 1.5; G42SK: undetermined, >50; K427D: 0.7, 0.03; G452K: 0.2, 0.8.

Table 2. Effect of Point Mutations of Pore-Associated Channel Residues on Expression and Block by TEA and CTX

Channel Position and Mutation	Functional Expression	CTX K_D(nM)	Ratio (mut/wt)	TEA K_D(mM)	Ratio (mut/wt)
Control	Yes	0.074 ± 0.004	=1	18.9 ± 0.7	=1
E418K	No				
A419K	Yes	0.069 ± 0.003	1.1	22.5 ± 0.3	1.2
G420K	Yes	0.40 ± 0.04	5	17 ± 3	1.1
S421K	Yes	0.58 ± 0.04	7.5	24 ± 1	1.3
E422K	Yes	1.50 ± 0.05	19	16.1 ± 0.2	1.2
N423K	Yes	0.91 ± 0.06	11	19 ± 2	1
S424K	Yes	1.8 ± 0.1	23	17.8 ± 0.2	1.1
G425K	Yes	200 ± 21	2500	48 ± 2	2.5
F426K	No				
K427D	Yes	0.0014 ± 0.001	.019	8 ± 1	2.4
S428K	No				
I429K	No				
P430K	No				
D431K	Yes	>250	>3125	22.4 ± 0.2	1.2
432-446	ND				
D44K	No				
M448K	Yes	67 ± 8	840	36 ± 1	1.9
T449K	Yes	>250	>3125	>200	11
T449D	No				
T449G	No				
T449A	Yes	0.39 ± 0.04	5	21 ± 2	1.1
T449S	Yes	0.27 ± 0.01	3.8	4.5 ± 0.3	3.8
P450K	ND				
V451K	Yes	>250	>3125	30 ± 1	1.6
G452K	Yes	0.12 ± 0.01	1.3	20 ± 1	1.1
V453K	Yes	0.28 ± 0.03	3.8	20 ± 2	1.1
W454K	Yes	0.19 ± 0.01	2.5	17.4 ± 0.8	1.1
G455K	No				
K456D	No				

The indicated channel position was mutated to lysine or aspartate, and CTX block was measured. Dissociation constants (K_D) for CTX and TEA with each channel mutant are tabulated as the mean ± SE for 3 or more determinations in separate oocytes; in a few cases, error bars represent the range of 2 determinations. ND, not done.

in the wild-type *Shaker* channel, which displays low affinity for CTX ($K_i \approx 120$ nM); throughout this study we have used as genetic background a point mutant at this position, F425G, that binds CTX with a 2000-fold enhanced affinity ($K_i \approx 70$ pM). Imagining that bound CTX may make close contact with the residue at 425, we analyzed replacements at this position with neutral hydrophobic residues of varying size (G, A, V, L, and F). Table 3 shows that, as expected, blocking affinity decreased with the size of the residue at *Shaker* position 425; the addition of even a single methyl group (G → A) led to a 6-fold loss of affinity. These effects were manifested wholly in increased toxin dissociation rates, with all mutants showing association rates close to wild-type values, ~5 x 10^7 $M^{-1}s^{-1}$. Thus, a bulky residue at position 425 appears to hinder CTX from fitting optimally on its receptor site.

Table 3. CTX Blocking Parameters for Channels with Position 425 Substitutions

Position 425 Amino acid	K_D (nM)	k_{on} ($\mu M^{-1}s^{-1}$)	k_{off} (s^{-1})
G	0.074 ± 0.004	61 ± 4	0.0046 ± 0.0003
A	0.43 ± 0.04	46 ± 6	0.018 ± 0.002
V	0.41 ± 0.02	40 ± 3	0.0163 ± 0.0006
L	160 ± 6	ND	ND
F	119 ± 6	67 ± 7	5.7 ± 0.5

CTX blocking parameters were determined in macropatches for channels carrying the residues indicated at position 425. Each value represents the mean ± SE for 4 or more independent determinations. ND, not done.

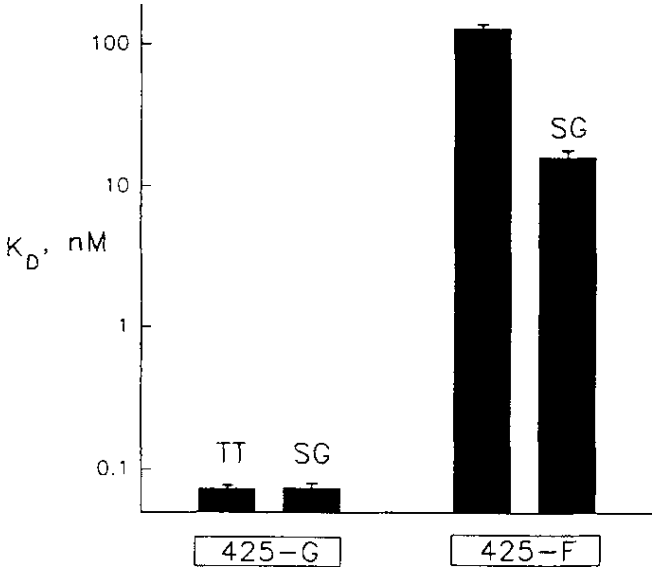

Figure 4. A CTX-Shaker Pair of Interacting Residues

Dissociation constants for 2 CTX variants and 2 *Shaker* variants were measured. Toxins differing in the residues at positions 8 and 9 were either wild-type CTX (TT) or T85+T9G (SG); channels differing in the residue at position 425 were either inactivation- removed Shaker (F) or F425G, (G). Association and dissociation rate constants, respectively, for the 4 toxin-channel combinations were as follows.

TT-425G: 61 ± 4 $\mu M^{-1}s^{-1}$, 0.0046 ± 0.0003 s^{-1}; SG-425G: 98 ± 6 $\mu M^{-1}s^{-1}$, 0.0071 ± 0.0004 s^{-1}; TT-425F: 50 ± 4 $\mu M^{-1}s^{-1}$, 7.3 ± 0.4s^{-1}; SG-425F: 50 ± 5 $\mu M^{-1}s^{-1}$, 0.85 ± 0.08 s^{-1}.

What part of the CTX molecule is involved in this destabilizing steric interaction with large residues at *Shaker*-425? Chimeras of CTX isotypes (data not shown) suggested that CTX residues TB and T9 might contribute to this interaction. These residues were individually "indifferent" when tested on the channel carrying a glycine at position 425 (Table 1); these "green" residues, which are indicated with black circles in Figure 2A, do not make direct contact with *Shaker*-F425G. However, they do appear to contact the CTX receptor of wild-type *Shaker*. Figure 4 compares the affinity of CTX with that of a double mutant, CTX-(T8S+T9G), in which these 2 threonines were replaced with smaller residues. This double mutation had no effect on toxin affinity when the channel bore a glycine at 425, as expected from the indifferent behavior of the individual single mutants. However, if the channel carried phenyalanine at 425, the TBS+T9G mutation affected the affinity; the double mutant bound 7-fold more tightly than did wild-type CTX, and this affinity difference was expressed entirely in the dissociation rate (Figure 4).

Our interpretation is that a bulky F425 on the channel makes unfavorable contact with T8 and T9 on bound CTX. We could completely eliminate this steric hindrance by greatly reducing the size of the channel residue (F → G); alternatively, we could ameliorate it by slightly lowering the volume of toxin residues (TT → SG). The double mutant toxin is still 200-fold weaker in absolute affinity on *Shaker*-425F than on *Shaker*- 425G; this result may simply reflect the fact that much more side chain volume is removed in the channel mutant (F → G) than in the toxin mutant (TT → SG), or that channel mutations appear 4 times in the homotetrameric complex, whereas toxin mutations are expressed only once. In any case, these experiments suggest that *Shaker* position 425 is located physically close (<5 Å) to residues 8 and 9 on bound CTX.

Discussion

In this study, we have tried to illuminate three aspects of the interaction of CTX with a *Shaker* K^+ channel. First, we have mapped the molecular surface of the toxin to locate the area making contact with the channel, as was done recently with a BK channel (Stampe et al., 1994). Second, using electrostatic point mutations, we have scanned the *Shaker* S5-S6 sequence to identify the important molecular determinants of the CTX receptor. Third, we have begun to identify toxin-channel interaction partners, to match up pairs of residues, 1 each on channel and toxin, that make close contact in the bound complex.

We rely heavily on kinetic analysis of CTX-*Shaker* interaction as the primary measurement on which interpretations are based. Broadly speaking, we view a residue as contributing to "close contact" if two criteria are satisfied. First, conservative replacement of the residue should lead to a large change in affinity. Second, much of this affinity change should be expressed in the CTX dissociation rate. A key feature of our analysis is its focus on the off-rate as a useful indicator of steric interactions between toxin and channel (Stampe et al., 1994); indeed, it is even more pertinent for this purpose than the equilibrium binding affinity itself, which reflects both steric and long-range electrostatic interactions.

These criteria are not a priori rigorous, but experience with several channels has shown them to be useful in developing predictive, self-consistent views of ion channel architecture (MacKinnon and Miller, 1989; Terlau et al., 1991; Satin et al., 1992; Backx et al., 1992; Heginbotham et al., 1992; Yang et al., 1993; Stampe et al., 1994). Moreover, the off-rate criterion is based on a sensible chemical kinetic argument (Park and Miller, 1992b). If a thermodynamically destabilizing mutation results in a greatly increased off-rate, then the free energy must be affected more in the bound complex than in the transition state between bound and free CTX. But only small configurational rearrangements are needed to achieve the transition state for these diffusion-limited, pore-blocking peptides; therefore, if the mutation alters the free energy of the bound state but not of the transition state, then a short-range, or "steric," interaction is operating. By the same logic, a purely long-range electrostatic interaction between distant residues is expected to affect both bound complex and transition state, and therefore should express itself in altered association rates (Bell and Miller, 1984; MacKinnon et al., 1989; Green and

Andersen, 1991; but see Escobar et al., 1993). In addition, since electrostatic potentials fall off quickly near protein interfaces, purely electrostatic mutations are expected to give smaller effects than close-contact mutations.

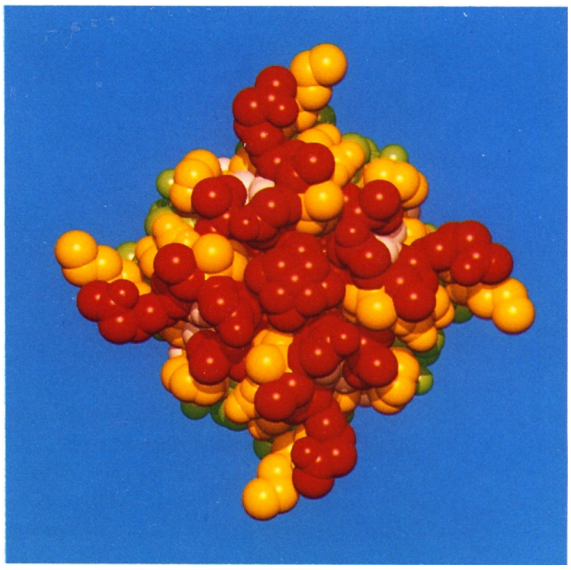

Figure 5. Fourfold Image of CTX Interaction Surface
The view of the CTX interaction surface shown in Figure 2D was repeated four times around a center of symmetry located on the ε-amino group of lysine 27. The figure was generated according to Stampe et al. (1994).

A Functional Map of the CTX Molecular Surface

A telling indicator of the validity of our approach is that the results produce a coherent physical picture of the toxin. All the residues scored as critical lie together, segregated from all those scored as indifferent (Figure 2). It is easy to imagine ways in which this clean result might not have emerged from the data, for instance, if point mutations at noncontact residues had produced even subtle conformational disruption of CTX. The clarity of the results implies that the point replacements are manifested locally and that the critical residues-those giving large off-rate changes when mutated-actually define a surface of close contact with the channel. This view is buttressed by the striking disposition of the weakly influential residues, which form a ring around the interaction surface, separating it from the indifferent residues. A "weak-contact" zone like this is expected if the critical residues define an area of close contact, and the indifferent residues de- fine the area of no contact.

The shape of the interaction surface is remarkably flat, at the resolution limited by uncertainty in side chain configurations of bound CTX (Stampe et al., 1994). There are no critical residues on the "sides" of the CTX molecule. Thus, the interaction surface, which covers the pore opening, implies a plateau-like receptor shape. The ring of weakly influential residues surrounds this flat surface at an only slightly higher elevation, 5-8 Å.

If the CTX interaction surface mirrors a complementary surface on the *Shaker* channel, we should be able to deduce the shape of the external opening of the channel. In picturing the shape of the CTX receptor, it is essential to remember that the channel is a fourfold symmetric structure, with the center of symmetry lying along the pore axis (MacKinnon, 1991; Heginbotham and MacKinnon, 1992; MacKinnon et al., 1993). The channel presents four equivalent configurations for CTX binding, only one of which may be occupied in a given channel-CTX complex. The deduction of the shape of this receptor requires correct placement of the channel's axis of symmetry on the CTX interaction sur face. Following identical arguments given for the BK channel (Stampe et al., 1994), we place the fourfold axis on CTX-K27, since it is known that the ε-amino group of this residue protrudes slightly into the K^+ conduction pore, where it interacts with conducting ions and also confers inherent voltage dependence on CTX dissociation (Goldstein and Miller, 1993). The channel surface is then envisioned by

reproducing the CTX interaction surface in fourfold symmetry about this point, adjusting the channel axis normal to the plane defined by CTX residues R25-K27-M29-N30-R34-Y36 (Stampe et al., 1994); this fourfold image of the toxin interaction surface is shown in Figure 5. It is very similar in shape to that derived for CTX interaction with a Ca^{2+}– activated K^+ channel (Stampe et al., 1994). The imagined complementary

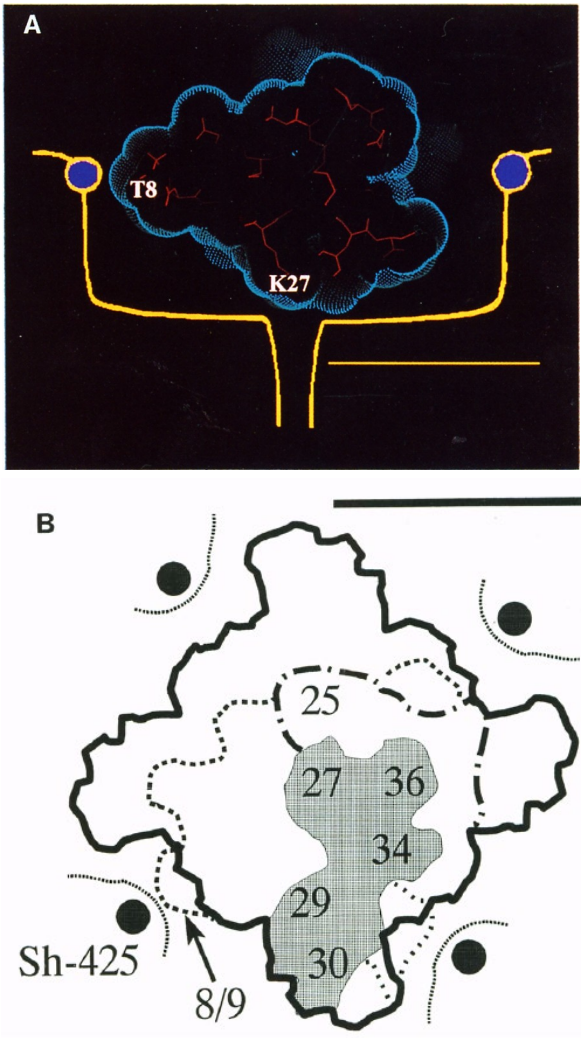

Figure 6. Localization of *Shaker*-425 in the Channel Vestibule
Schematic views of CTX bound to the deduced shape of the CTX receptor were produced from manipulation of CTX coordinates (Bontems et al., 1992) in the QUANTA molecular graphics program. Sections ~1 Å thick were examined to locate positions of pertinent residues. Scale bars of 20 Å are displayed. (A) A vertical section through CTX (solvent-accessible surface shown as blue dots) was taken through the proposed channel axis (intersecting CTX-K27) and the β-carbon of T8. (In this view, T9 lies behind the displayed section, adjacent to T8.) Orientation of the toxin was achieved by y-axis rotation of the view of Figure 2A by +80°. Approximate positions for *Shaker*-425 are indicated by bright blue blobs, assuming close proximity to CTX-T8. (B) Aerial view of the CTX receptor. Sections normal to the pore axis were taken of the proposed fourfold receptor interaction area (Figure 5), at the level of the receptor floor (heavy outline). The figure also displays the orientation of a single bound CTX molecule on the receptor, with positions of pertinent residues indicated by number. Gray shaded area: footprint of close- contact residues at level of receptor floor (zero elevation). Dashed outline: footprint weak-contact residues at zero elevation. Dotted outline, projected "shadow" of entire CTX molecule. Projected positions of CTX-T8/T9, which lie at 12 A elevation, are also indicated, as are the proposed locations for *Shaker*-425 at this elevation.

surface of the channel argues that the narrow K^+ conduction pore abruptly widens at the external solution to a flat pinwheel-shaped plateau of dimensions 25 x 35 Å. This outer opening is neither deeply cup-shaped nor funnel-shaped, nor is there any evidence for a high wall or "mouth," as is known to exist, for example, in the nicotinic acetyl- choline receptor channel (Unwin, 1993). We will see below, however, that a low wall exists slightly beyond the radial extent of this receptor plateau.

CTX Receptor Determinants in the Shaker Channel

The *Shaker* channel, like numerous voltage-gated and Ca^{2+}-activated K^+ channels, carries a receptor for CTX family peptides near the outer opening of the pore. CTX itself binds weakly to the wild-type *Shaker* channel ($K_i \approx 120$ nM), but this affinity may be strengthened 2000-fold by the single point mutation F425G. Previous studies using a CTX isoform (MacKinnon et al., 1990) identified residues in the S5-S6 linker that specifically influence toxin binding. We have now scanned this same region by replacing residues with lysine, which is expected to destabilize electrostatically the binding of the positively charged CTX molecule. Nearly all the lysine mutations act in this way; those far from the pore-forming P-region (Figure 3) destabilize weakly, whereas those near the pore are much stronger in their influence. We share the view of MacKinnon and coworkers (1990), that the weak residues, which influence mainly association rates and whose effects are sensitive to ionic strength, operate via distant electrostatic interactions, whereas close-range forces dominate the residues near the P-region. The transition from "weak" to "strong" positions occurs with remarkable suddenness in the channel sequence, at positions 424-425 and 451-452, as though the steric footprint of CTX covers the strong residues, whereas the weaker positions lie farther away, in the toxin's electrostatic shadow.

We also replaced the naturally occurring lysine (K427) with an aspartate and observed an additional 50-fold strengthening of CTX affinity ($K_i \approx 1.5$ pM), most of which is expressed in a lowered dissociation rate. Thus, a double mutant *Shaker* channel, F425G+ K427D, displays a receptor 10^5-fold improved in CTX affinity over wild-type *Shaker*; the time constant of toxin wash-off from this double mutant channel is greater than 2 hr at room temperature. This construct offers an impressive example of the participation of both close-range steric and long-range electrostatic forces in the recognition of CTX by its receptor.

A Search for Interaction Partners

A compelling motivation for studying the CTX-*Shaker* interaction is the hope that the known structure of the toxin might suggest structural features of the K^+ channel. The identification of channel residues making contact with known CTX residues would be particularly valuable, since several such interaction partners would permit physical triangulation of distances between specific channel residues. In searching for such contact-pairs, we first attempted to identify salt bridges between basic toxin and acidic channel residues; to do this, we assayed all combinations of charge-reversed pairs, in hopes of hitting upon complementary mutations. These efforts were complete failures; we could not find any such complementary charge-reversed pairs of residues.

Nevertheless, we have identified 2 CTX residues, T8 and T9, that appear to interact sterically with *Shaker*- F425. When the channel carries a large residue (F or L) at position 425, CTX binds poorly; this binding may be strengthened about an order of magnitude by mutating T8 and T9 to smaller residues, S and G, respectively. When the channel carries a small residue at position 425, however, CTX-T8T9 and CTX-S8G9 bind with precisely identical, and much stronger, affinities. We take this result as evidence for a destabilizing contact between F425 on the channel and the T8-T9 area on the toxin; reducing the residue volume on the toxin leads to less steric hindrance. When F425 is made smaller by several angstroms, this destabilizing contact is lost, the toxin binds strongly, and the binding is no longer sensitive to the size of the residues on the toxin. This picture is further supported by the observation that CTX binding is systematically weakened as the size of the residue at *Shaker*-425 increases (Table 3).

Where are the toxin positions T8 and T9 located in space? These are both green residues on the toxin surface and are explicitly indicated in Figure 2A, positioned above the interaction plateau that

forms the bottom of the toxin (Figure 5). Figure 6A presents a vertical section through the receptor-bound toxin, in the plane defined by the channel axis (hence CTX-K27) and CTX-T8. The residues T8 and T9 protrude 13-15 Å radially out from the pore axis about 12 Å above the floor of the CTX receptor. This geometry places *Shaker*-425 at a straight-line distance of ~20 Å from the point of intersection between the axis of symmetry and the abrupt external opening of the pore. We conclude from this analysis that *Shaker*-425 is not located on the pinwheel-shaped plateau deduced from the CTX interaction surface, but rather on a "wall" (or possibly one of four “hills”) surrounding this plateau. In wild-type *Shaker*, the wall makes unfavorable contact with CTX, but in *Shaker*-F425G this contact is lost, and the affinity becomes high. The CTX receptor of the BK channel also displays a similar wall, but for this channel the wall contributes contacts that favor toxin binding (Stampe et al., 1994).

Figure 6B summarizes in cartoon form the physical features we have deduced here for the CTX receptor, as viewed from the external side of the membrane. The heavy curve outlines the fourfold plateau (Figure 5) at the level of the pore opening, with CTX-K27 on the symmetry axis. The gray area represents the close-contact footprint of a single CTX molecule, while the dashed curve outlines the weak-contact residues surrounding the plateau-level footprint. Deduced positions of the four *Shaker*-425 residues are also indicated at an elevation of ~12Å above the receptor floor. One of these residues is in close proximity with CTX-T8/T9, while the other 3 are farther removed from the surface of bound CTX. It will be important in future work to identify additional CTX-*Shaker* interaction partners so that our physical picture of the channel's outer end, which is palpably vague, can be brought into sharper focus.

Experimental Procedures

Biochemical Methods

Production of Recombinant CTX Variants

CTX and mutant variants were produced in Escherichia coli as cleavable fusion proteins and purified as previously described (Park et al.,1991). Each mutant met previously established criteria for correct folding (Stampe et al., 1994) based on chromatographic profiles, integrity of blocking mechanism, and behavior when assayed on single Ca^{2+}- activated K+ channels. In addition, 2 variants (Y36A and K27Q) with exceptionally low affinity were confirmed to have native backbone folding pattern by two- dimensional NMR.

Production of Shaker K^+ Channel Mutants

The CTX-sensitive, inactivation-removed *Shaker* K^+ channel (Δ6-46/F425G) used here has been described (Goldstein and Miller, 1992, 1993). Residues are numbered according to wild-type *Shaker* B (Schwarz et al., 1988). To expedite mutation of the CTX receptor, we constructed convenient restriction sites in a *Shaker* B cDNA, kindly supplied by Dr. R. MacKinnon, carrying a deletion of inactivation domain residues 6-46 (Hoshi et al., 1990). A single round of site-directed mutagenesis on single-stranded DNA was performed using 7 mutagenic primers to create 1 amino acid replacement, F425G, and 6 "silent" changes that altered restriction enzyme sensitivity but not protein sequence. The silent changes removed a BamHI site in the coding sequence at G124, an Accl site at R146, and an Accl site in the Bluescript KS+ polylinker region; silent changes added an Accl site at the coding sequence for V414 (in S5), a BamHI site at G459 (in S6), and an Ncol site at the initiation ATG. The new Accl and BamHI sites permitted easy replacement of the S5-S6 linker with mutagenic cassettes. Mutant Accl-BamHI fragments were produced either by single-stranded or polymerase chain reaction mutagenesis. All mutations were confirmed bydideoxy sequencing, and cRNA was prepared using T7 RNA polymerase (Promega) supplemented with capping nucleotide after linearization with HindIII.

Electrophysiology

Xenopus oocytes were injected with 5 ng of cRNA for macropatch recording and 0.05 ng of cRNA for whole-oocyte studies. Currents were recorded from outside-out patches without leak subtraction using an Axopatch 1-C (Axon Instruments) or an Oocyte Clamp (Warner Instruments). Bath

solution was 2 mM KCI, 100 mM NaCl, 1 mM MgCI,, 0.3 mM CaCI,, 10 mM HEPES (pH 7.1), 25 µg/ml bovine serum albumin. Internal pipette solution for patch electrodes was 100 mM KCI, 1 mM MgCI,, 5 mM EGTA, 10 mM HEPES (pH 7.1); for intracellular electrodes, internal pipette solution was 3 M KCI. All experiments were performed at 21°C-23°C. When a point mutation failed to express K^+ currents, the negative result was confirmed by repeated cRNA synthesis and injection of 100-fold higher levels of cRNA.

Macropatches expressing 0.5-2.5 nA of K^+ current were moved into a rapid exchange perfusion chamber as previously described (Goldstein and Miller,1993). For each toxin variant, kinetics were measured in at least 4 patches surviving a complete wash-in/wash-out cycle and recovering to within 5% of control current levels. Such criteria are difficult to achieve with wild-type dissociation rates, since each patch must last over 20 min. In this work, therefore, some CTX variants with slow dissociation rates were first tested in several macropatches and subsequently recorded with whole-oocyte clamp, which provides stable current levels for many hours. Fast fluid exchange (~10 ms) for patch experiments was driven by acomputer-controlled, gravity-flow system. Fluid exchange for whole-oocyte experiments was complete in ~5 s. Blocking experiments were performed as previously described (Goldstein and Miller, 1993). Briefly, solution flow was constant during both control and blocking pulses. Wash-in: after 4 control pulses with toxin-free solution, the solution was changed to one containing toxin (at about twice the K_D), and brief test pulses were applied until equilibrium blockade was reached. Wash-out: after 4 control pulses at equilibrium in the presence of toxin, toxin-free solution was switched in, and pulses were applied until full recovery. Time constants were determined by single-exponential fits. Single-pulse experiments allow observation of the kinetics of channel blockade within a single 450 ms sweep and were performed for toxin variants with rapid off-rates as described (Goldstein and Miller,1993). Kinetics of K^+ channel inhibition by CTX are known to follow a bimolecular blocking scheme (Anderson et al., 1988; Goldstein and Miller, 1993; Escobar et al., 1993):

$$\text{Channel} + \text{CTX} \underset{k_{off}}{\overset{k_{on}}{\rightleftharpoons}} \text{Channel:CTX}$$

Association and dissociation rate constants, k_{on} and k_{ofl}, are readily determined from the wash-in time constant and the equilibrium fraction of unblocked current (Goldstein and Miller, 1993). The wash-out time constant directly measures the dissociation rate constant and thus serves as an internal check on the kinetic parameters. For this scheme, the inhibition constant (K_i), measured from the equilibrium unblocked current, is rigorously equal to the equilibrium dissociation constant of toxin (K_D).

Acknowledgments

We thank P. Stampe and L. Kolmakova-Partensky for some CTX preparations, M. Stocker for determining the kinetic parameters of mutants T8K and T9K, and D. Peisach for molecular graphics. This research was in part supported by National Institutes of Health grant #HL-02770.

The costs of publication of this article were defrayed in part by the payment of page charges. This article must therefore be hereby marked "advertisement" in accordance with 18 USC Section 1734 solely to indicate this fact.

Received February 18, 1994; revised April 11, 1994.

References

Anderson, C., M acKinnon, R., Smith, C., and Miller, C. (1988). Charybdotoxin inhibition of Ca^{2+}-activated K^+ channels. Effects of channel gating, voltage, and ionic strength. J. Gen. Physiol. 91, 317-333.

Backx, P. H., Yue, D. T., Lawrence, J. H., Marban, E., and Tomaselli, G. F. (1992). Molecular localization of an ion-binding site within the pore of mammalian sodium channels. Science 257, 248-251.

Bell, J. E., and Miller, C. (1984). Effects of phospholipid surface charge on ion conduction in the K^+ channel of sarcoplasmic reticulum. Biophys. J. 45, 279-288.
Bontems, F., Roumestand, C., Bayot, P., Gilquin, B., Doljansky , Y., Menez , A., and Toma, F. (1991). Three-dimensional structure of natural charybdotoxin in aqueous solution by ^{1}H-NMR. Eur. J. Biochem. 196, 19- 28.
Bontems, F., Gilquin, B., Roumestand, C., Menez, A., and Toma, F. (1992). Analysis of side-chain organization on a refined model of charybdotoxin: structural and functional implications. Biochemistry 31, 7756-7764.
Candia, S., Garcia, M. L., and Latorre, R. (1992). Mode of action of iberiotoxin, a potent blocker of the large conductance Ca^{2+}- activated K^+ channel. Biophys. J. VOLUME?, 583-590.
Crest, M., Jacquet, G., Gola, M, Zerrouk, H., Benslimane, A., Ro chat, H., Mansuelle, P., and Martin-Eauclaire, M. (1992). Kaliotoxin, a novel peptidyl inhibitor of neuronal BK-type Ca^{2+}- activated K^+ channels characterized from *Androctonus mauretanicus mauretanicus* venom. J. Biol. Chem. 267, 1640-1 647.
Escobar, L., Root, M. J., and MacKinnon, R. (1993). Influence of protein surface charge on the bimolecular kinetics of a potassium channel peptide inhibitor. Biochemistry 32, 6982-6987.
Garcia-Calvo, M., Leonard, R. J., Novick, J., Stevens, S. P., Schmalhofer, W., Kaczorowski, G. J., and Garcia, M. L. (1993). Purification, characterization, and biosynthesis of margatoxin, a component of *Centruroides mararitatus* venom that selectively inhibits voltage-dependent potassium channels. J. Biol. Chem. 268, 18866- 18874.
Garcia, M. L., Garcia-Calvo, M., Hidalgo, P., Lee, A., and MacKinnon, R. (1994). Purification and characterization of three inhibitors of voltage-dependent K^+ channels from *Leiurus quinquestriatus hebreus* venom. Biochemistry, in press.
Giangiacomo, K. M., Garcia, M. L., and McManus, 0. B. (1992). Mechanism of iberiatoxin block of the large-conductance calcium-activated potassium channel from bovine aortic smooth muscle. Biochemistry 31, 6719-6727.
Gimenez-Gallego, G., Navia, M. A., Reuben, J. P., Katz, G. M., Kaczorowski, G. J., and Garcia , M. L. (1988). Purification, sequence, and model structure of charybdotoxin, a potent selective inhibitor of calcium-activated potassium channels. Proc. Natl. Acad. Sci. USA 85, 3329-3333.
Goldstein, S. A. N., and Miller, C. (1992). A point mutation in a *Shaker* K^+ channel changes its charybdotoxin binding site from low to high affinity. Biophys. J. 62, 5-7.
Goldstein, S. A. N., and Miller, C. (1993). Mechanism of charybdotoxin block of a *Shaker* K^+ channel. Biophy s. J. 65, 1613-1619.
Green, W. N., and Andersen, O. S. (1991). Surface charges and ion channel function. Annu. Rev. Physiol. 53, 341- 3.59.
Heginbotham, L., and MacKinnon, R. (1992). The aromatic binding site for tetraethylammonium ion on potassium channels. Neuron 8, 483- 491.
Heginbotham, L., Abramson, T., and MacKinnon, R. (1992). A functional connection between the pores of distantly related ion channels as revealed by mutant K^+ channels. Science 258, 1152- 1155.
Hoshi, T., Zagotta, W. N., and Aldrich, R. W. (1990). Biophysical and molecular mechanisms of *Shaker* potassium channel inactivation. Science 250, 533-538.
MacKinnon, R. (1991). Determination of the subunit stoichiometry of a voltage-activated potassium channel. Nature 500, 232- 235.
MacKinnon, R., and Miller, C. (1988). Mechanism of charybdotoxin block of Ca^{2+}-activated K^+ channels. J. Gen. Physiol. 91, 335- 349.
MacKinnon, R., and Miller, C. (1989). Mutant potassium channels with altered binding of charybdotoxin, a pore-blocking peptide inhibitor. Science 245, 1382-1385.
MacKinnon, R., and Yellen, G. (1990). Mutations affecting TEA blockade and ion permeation in voltage-activated K^+ channels. Science 250, 276-279.
MacKinnon, R., Latorre, R., and Miller, C. (1989). Role of surface electrostatics in the operation of a high-conductance Ca^{2+}- activated K^+ channel. Biochemistry 28, 8092-8099.

MacKinnon, R., Heginbotham, L., and Abramson, T. (1990). Mapping the receptor site for charybdotoxin, a pore-blocking potassium channel inhibitor. Neuron 5, 767-771.
MacKinnon, R., Aldrich, R. W., and Lee, A. W. (1993). Functional stoichiometry of *Shaker* potassium channel inactivation. Science 262, 757-759.
Miller, C. (1988). Competition for block of a Ca^{2+}-activated K^+ channel by charybdotoxin and tetraethylammonium. Neuron 1, 1003-1006.
Miller, C. (1991). 1990: annus mirabili s of potassium channels. Science 252, 1092-1096.
Miller, C., Moczydlowski, E., Latorre, R., and Phillips, M. (1985). Charybdotoxin, a high-affinity inhibitor of single Ca^{2+}-activated K^+ channels of mammalian skeletal muscle. Nature 313, 316-318.
Park, C. S., and Miller, C. (1992a). Interaction of charybdotoxin with permeant ions inside the pore of a K^+ channel. Neuron 9, 307-313.
Park, C. S., and Miller, C. (1992b). Mapping function to structure in a channel-blocking peptide: electrostatic mutants of charybdotoxin. Biochemistry 31, 7749-7755.
Par k, C. S., Hausdorff, S. F., and Miller, C. (1991).Design, synthesis, and functional expression of a gene for charybdotoxin, a peptide blocker of K^+ channels. Proc. Natl. Acad. Sci. USA 88, 2046- 2050.
Possani, L. D., Martin, B. M., and Svendensen , I. (1982). Calsberg Res. Commun. 47, 285-289.
Satin, J., Kyle, J. W., Chen, M., Bell, P., Cribbs, L. L., Fozzard,
H. A., and Rog art, R. B. (1992). A mutant of TTX-resistant cardiac sodium channels with TTX-sensitive properties. Science 256, 1202-1205.
Schwarz, T. L., Tempel, B. L., Papazian, D. M., Jan, Y.-N., and Jan, L.-Y. (1988). Multiple potassium-channel components are produced by alternative splicing at the *Shaker* locus in *Drosophila*. Nature 331, 137-142.
Stampe, P., Kolmakova-Partensky, L., and Miller, C. (1994). Intimations of K^+ channel structure from a complete functional map of the molecular surface of charybdotoxin. Biochemistry 33, 443- 450.
Terlau, H., Heinemann, S. H., Stuhmer, W., Pusch, M., Conti, F., Imoto, K., and Numa, S. (1991). Mapping the site of block by tetrodotoxin and saxitoxin of sodium channel II. FEBS Lett. 293, 93-96.
Unwin, N. (1993). Nicotinic acetylcholine receptor at 9Å resolution. J. Mol. Biol. 229, 1101-1124.
Yang, J., Ellinor, P. T., Sather, W. A., Zhang, J. F., and Tsien, R. W. (1993). Molecular determinants of Ca^{2+} selectivity and ion permeation in L-type Ca^{2+} channels. Nature 366, 158-161.